Direct measurement of fungal contribution to silicate weathering rates in soil

Bastien Wild[1,2]*, Gwenaël Imfeld[2] and Damien Daval[2]

[1]Andlinger Center for Energy and the Environment, Princeton University, Princeton, New Jersey 08544, USA
[2]Institut Terre et Environnement de Strasbourg, Université de Strasbourg, ENGEES, CNRS, UMR 7063, 5 rue Descartes, Strasbourg 67000, France

ABSTRACT

Chemical weathering produces solutes that control groundwater chemistry and supply ecosystems with essential nutrients. Although microbial activity influences silicate weathering rates and associated nutrient fluxes, its relative contribution to silicate weathering in natural settings remains largely unknown. We provide the first quantitative estimates of *in situ* silicate weathering rates that account for microbially induced dissolution and identify microbial actors associated with weathering. Nanoscale topography measurements showed that fungi colonizing olivine $[(Mg,Fe)_2SiO_4]$ samples in a Mg-deficient forest soil accounted for up to 16% of the weathering flux after 9 mo of incubation. A local increase in olivine weathering rate was measured and attributed to fungal hyphae of *Verticillium* sp. Altogether, this approach provides quantitative parameters of bioweathering (i.e., rates and actors) and opens new avenues to improve elemental budgets in natural settings.

INTRODUCTION

A next frontier in quantitative modeling of silicate weathering in the critical zone, where "rocks meet life" (Brantley et al., 2011), is the incorporation of microbial activity in reactive transport models (RTMs; Frings and Buss, 2019; Goddéris et al., 2019). Microorganisms contribute to the transformation of rock to regolith (Napieralski et al., 2019), and microbially mediated weathering fluxes of silicates may have been critical for the habitability of Earth (Schwartzman and Volk, 1989). This process could also impact the development of carbon capture and storage strategies based on silicate dissolution, such as enhanced rock weathering (Beerling et al., 2020). However, the contribution of microorganisms to silicate weathering in natural settings remains uncertain (Frings and Buss, 2019).

Microorganisms owe their survival to their ability to scavenge elements with low solubility and/or concentration, or trace metals used as enzyme cofactors, for which minerals may be the unique source (Banfield et al., 1999). Echoing the paradigm proposed by Hazen et al. (2008), the coevolution of the geo- and biospheres may favor microbial communities specifically adapted to each mineral surface, possibly harboring microorganisms with efficient weathering ability (Uroz et al., 2015). Microenvironments are generated at the silicate-microbe interface (Benzerara et al., 2005), where locally aggressive conditions can remarkably increase silicate weathering rates (Bonneville et al., 2009; Li et al., 2016), as reported in numerous laboratory experiments involving microbial cultures (Uroz et al., 2015). However, quantitative upscaling of laboratory results to natural settings is not straightforward.

On the one hand, laboratory experiments are not designed to be fully representative of natural environments. These experiments generally use synthetic media, which purposely stimulate microbial growth and/or bioweathering, and result in higher microbially mediated mineral dissolution rates than under field conditions. In addition, the commonplace use of axenic strains cannot account for the interplay between distinct populations in a microbial community and its effect on mineral dissolution rates.

On the other hand, probing microbial weathering in the field is challenging. Concentrations in soil solution of biomolecules promoting silicate dissolution, such as organic acids (OAs), are frequently argued to be too low in natural settings to increase the dissolution rate beyond the microbe-mineral contact (Drever and Stillings, 1997). While most estimates of microbially mediated silicate weathering rates so far have been derived from laboratory experiments (Wild et al., 2018), a few pioneering studies have provided environmental estimates for naturally altered minerals in surface aquifers (Rogers and Bennett, 2004) or soil profiles (e.g., van Schöll et al., 2008, and references therein) based on scanning electron microscopy (SEM) analysis. However, current approaches are not suited to quantify the actual mineral volume dissolved by microorganisms such as fungi and fail to provide a simultaneous measurement of the fungal-free contribution to the overall dissolution rate *in situ*. As a result, clear imprints of bioweathering often remain subtle and controversial (Knowles et al., 2012), while models predicting mineral dissolution and associated carbon and nutrient budgets overlook the contribution of microbial actors, which remains essentially unknown.

We developed an approach to directly quantify *in situ* mineral weathering rates in natural environments, providing a joint evaluation of the fungal contribution to the overall weathering flux and the associated fungal diversity. Our approach relies on the *in situ* incubation of well-characterized mineral samples, which circumvents the aforementioned limitations by ensuring a representative biogeochemical environment while providing quantitative rate estimates. It combines an interpretation of the nanoscale topography of mineral surfaces resulting from weathering (Kirtzel et al., 2017; Fischer and Luttge, 2018) with an analysis of associated microbial taxa using DNA–based high-throughput sequencing (Jones and Bennett, 2014). Olivine samples were incubated for 9 mo in the A horizon of a Mg-deficient forest soil to probe its weathering potential. The incubation of basaltic minerals in base-poor soils has been recently acknowledged as a promising strategy

*E-mail: bwild@princeton.edu

to stimulate enhanced rock weathering for carbon dioxide removal (Beerling et al., 2020). However, the biotic and abiotic contributions to the overall weathering rate have not yet been experimentally teased apart in natural settings, partly due to the complexity in obtaining an abiotic reference point that does not exist on Earth today (Frings and Buss, 2019). Cross-correlations of optical microscopy images with vertical scanning interferometry (VSI) topography data provided the first *in situ* quantification of mineral dissolution rates together with estimates of the fungal contribution to the overall weathering rate. These results were coupled with fungal diversity data to identify potential fungal taxa associated with bioweathering. Altogether, this approach provides a long sought-after framework for benchmarking quantitative reaction models while incorporating microbially driven weathering.

METHODS

Olivine samples were prepared both as crushed powders (160–315 μm) and polished monoliths (~5 mm on a side), packed into nylon bags, and sterilized in ethanol. The nylon bags were buried for 9 mo into the A horizon of a Mg-deficient forest soil (beech plot) developed on a Hercynian base-poor granite located in the Strengbach catchment, Aubure, France (48°12′41.04″N, 7°11′45.66″E) (Pierret et al., 2018). The plot chosen for this study was part of an instrumented site of the Observatoire Hydro-Géochimique de l'Environnement (OHGE) critical zone observatory, which enabled us to retrieve environmental parameters monitored on site during sample incubation. Olivine was purposely selected because it has recently been proposed as an additive to promote enhanced weathering in Mg-deficient soils. The average pH of soil solution was 4.2 ± 0.2, and concentrations of the most common low-molecular-weight OAs (acetate, formate, malonate, oxalate, citrate) measured by ion chromatography (ICS 3000 DIONEX) were below the detection limit (<5 mmol/L). The temperature of the soil varied between 25 °C and −9 °C, and the average precipitation was ~125 mm/mo over the incubation period.

Monolith samples were visualized with reflected light microscopy and SEM (Tescan® VEGA II). Materials adhering to the surface were then mechanically and chemically removed using cotton swabs, ethanol, and acetone. The difference in nanotopography between weathered and unweathered regions of the olivine surface masked with a room-temperature vulcanizing (RTV) glue spot was measured using VSI (Zygo NewView 7300), from which rate maps were extracted as described in Fischer and Luttge (2018). Subsequent transformation of rate data from the spatial domain to the frequency domain was used to generate rate spec-

tra (Fischer and Luttge, 2018), from which rate contributors were identified.

After 9 mo, total DNA was extracted with a PowerSoil® DNA Isolation Kit (MO BIO, Carlsbad, California, USA) both from the olivine powder samples and the surrounding soil. DNA was quantified with a Qubit 2.0 spectrofluorometer (Life Technologies, Grand Island, New York, USA). Fungal diversity was evaluated for each sample by targeting the internal transcribed spacer 2 (ITS2) region of the 18S ribosomal ribonucleic acid (rRNA) gene, amplified using a standardized 18S amplicon library protocol as previously described by, e.g., Al-Bulushi et al. (2017). Gene sequences were analyzed by Genoscreen Laboratory (Lille, France) using a standard analysis pipeline (Al-Bulushi et al., 2017). Sequencing data obtained after treatment and classification were used to examine the fungal community composition. Fungal enrichment at the genus level was estimated based on the ratio of the relative abundance of the fungal genus associated with the olivine sample ($n_{olivine}$) to the relative abundance of the fungal genus in soil (n_{soil}).

DNA sequences were deposited in the National Center for Biotechnology Information (NCBI) BioProject database and are freely accessible through the NCBI website (https://www.ncbi.nlm.nih.gov/bioproject/638437).

RESULTS AND DISCUSSION

Optical microscopy and SEM analyses showed abundant filaments on the olivine samples (Fig. 1A), typical of colonization by fungal hyphae (e.g., van Schöll et al., 2008).

SEM and VSI analyses evidenced depressions located underneath the hyphae after their removal, such as those shown in Figures 1B and 2A (green arrows). These features were absent from the initial minerals and contrasted with crystallographically controlled etch pits (Fig. 1B, black arrows) typical of abiotic weathering of olivine (Velbel, 2009). They were thus interpreted as the result of local bioweathering.

VSI measurements of the surface topography indicated that the average depth of fungi-associated depression was 235 ± 125 nm; after conversion to a local dissolution rate, this corresponds to $2.2 \pm 1.2 \times 10^{-10}$ moles of olivine per square meter per second ($mol/m^2/s$). This value does not consider the potential contribution of solid-state leaching through an amorphous silica-rich layer, as suggested, for instance, for biotite-fungi interactions by Bonneville et al. (2011). Arguably, such amorphous layers are very thin (≤ 5 nm) on olivine weathered at ambient temperature (Hellmann et al., 2012) and might even be absent at the fungus-olivine interface (Gerrits et al., 2021). This contribution can therefore be neglected.

In contrast, the average value of surface retreat for the whole sample was 23 ± 2 nm (dissolution rate of $2.2 \pm 0.2 \times 10^{-11}$ mol/m²/s), reflecting olivine weathering resulting from the interaction between the bulk soil solution and olivine, without direct fungal contribution. Taken together, the magnitude of enhanced dissolution under the fungal hyphae (~10-fold factor) is very similar to the estimation by Bonneville et al. (2011) from laboratory experiments with biotite.

Rate spectra analysis (Fig. 2B) helped to tease apart biotic and abiotic contributions to the overall dissolution rate. Two clusters of peaks can be distinguished from the reference surface (yellow in Fig. 2B). They correspond to rate contributions of the fungal-free portion of the surface impacted by fluid-mineral interactions (blue in Fig. 2B), and to fungus-related weathering (green in Fig. 2B). The latter cluster exhibited faster average rates with smaller integral (due to smaller surface area) and included several rate contributors likely related to the evolution of the spatial extent of fungal weathering. Interestingly, the overall dissolution rate was lower than rates estimated with RTMs based on environmental parameters (fluid composition, soil temperature) recorded at this location during sample incubation (~10–20 times lower depending on the model chosen; for more
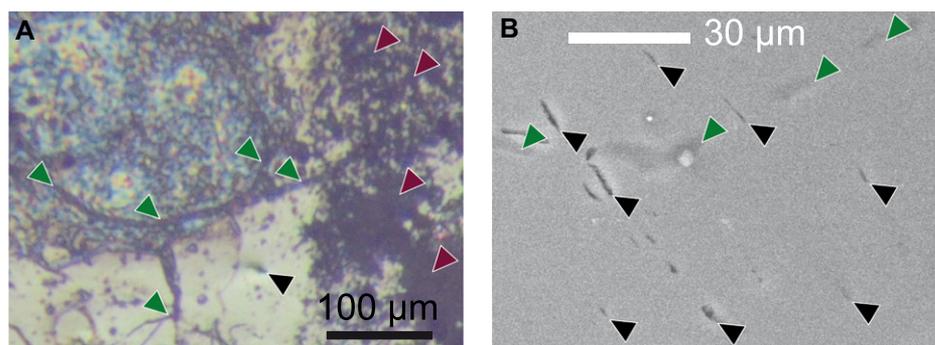

Figure 1. Surface of olivine samples after incubation in forest soil. (A) Reflected light microscopy showing hyphae colonization (green arrows) at the surface of the olivine sample in the middle of clay and organic matter deposits (purple arrows) and etch pits (black arrows). (B) Scanning electron microscope (SEM) image of portion of mineral surface showing abiotic etch pits (black arrows) and depressions related to the action of fungal hyphae (green arrows).

A

z [nm]

Reference Surface

Altered Surface

y [μm]

x [μm]

B

Log [frequency]

Solution-related flux

Fungus-related flux

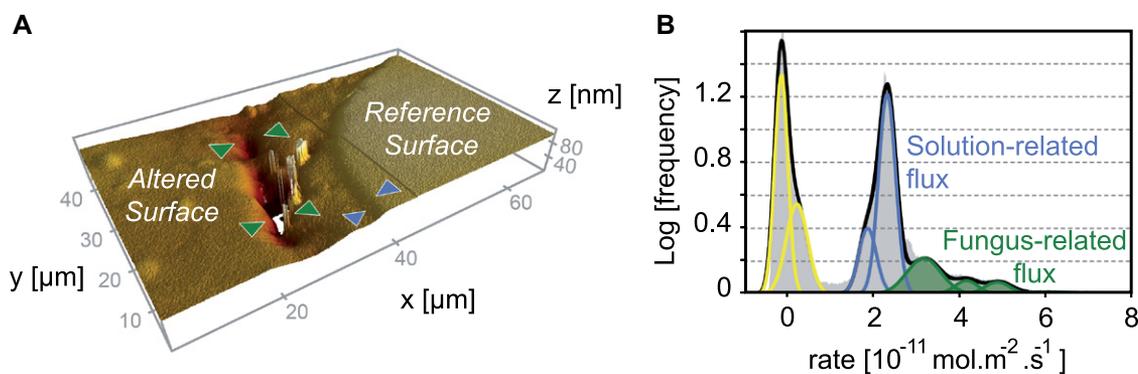rate [10^{-11} mol.m^{-2}.s^{-1}]

Figure 2. (A) Three-dimensional vertical scanning interferometry (VSI) image showing global surface retreat (blue arrows) and depression resulting from fungal weathering (green arrows), where *z* axis is expanded relative to *x* and *y* axes according to instrument's resolution. (B) Corresponding rate spectrum (gray shading), fit (black curve), reference surface (yellow), and associated rate contributors, including "abiotic" (blue) and "biotic" (green) processes.

discussion on this discrepancy, see Wild et al. [2019]). Those simulations were based on state-of-the-art kinetic parameters and did not include any bioweathering component. This emphasizes the observation that microbial weathering is insignificant in areas devoid of hyphae, which would otherwise tend to increase rates compared to abiotic estimates.

Fungal-mediated fluxes accounted for up to 16% of the dissolution flux over 9 mo, as estimated from a portion of the olivine surface area colonized by fungi. This estimation falls within the range of values previously reported using indirect methods (0.5%–50%; see van Schöll et al., 2008). It probably represents a lower bound, since fungal colonization of olivine likely did not reach a steady state. Our results show that possible fungal contribution to the dissolution process is spatially limited to the close vicinity of hyphae in contact with the mineral surface, consistent with the importance of surface attachment in microbial weathering processes highlighted in previous studies (Bonneville et al., 2011; Ahmed and Holmstrom, 2015; Gerrits et al., 2021). Moving forward, evaluation of the spatial heterogeneity related to, for example, mineral surface coverage by microorganisms and assessments of its temporal evolution will constitute key steps in the formulation, parameterization, and validation of "microbially informed" RTMs (Meile and Scheibe, 2019). This can be achieved by extending approaches combining surface imaging with surface topography analysis, such as developed in the present study, to larger sets of samples including time series. Moreover, the extent of local silicate weathering was related to potential fungal actors. Relating reaction rates, microbial community composition, and, ultimately, their functional traits is another prerequisite to further develop RTMs that explicitly represent microorganisms (Meile and Scheibe, 2019). The fungal diversity associated with the olivine samples differed from that of the bulk soil, with the specific enrichment in a limited number of genera compared to the surrounding soil (Fig. 3). This echoes previous studies suggesting that single minerals represent a specific ecological niche for bacteria (Mitchell et al., 2013; Jones and Bennett, 2014; Uroz et al., 2015) and fungi (Gleeson et al., 2005). The main fungal genera, most likely corresponding to the hyphae observed by optical microscopy, were *Hydnotrya* (14.3%), *Mortierella* (12.0%), and *Verticillium* (4.4%) (Fig. 1A). In particular, some members of the most enriched genus at the olivine surface, i.e., *Verticillium* (cf. Fig. 3), are capable of synthesizing OAs and siderophores and can weather Mg-silicates (Daghino et al., 2009). Chemotaxis might be a major mechanism that promoted olivine colonization and subsequent dissolution by fungal hyphae, since olivine samples were incubated in a Mg-deficient soil compartment (Wild et al., 2019).

Species belonging to the *Verticillium* genus (Fig. 3) may thus be associated with high-dissolution-rate features (Fig. 2B) and may be involved in silicate weathering and CO_2 drawdown when stimulated with the appropriate silicate substrates. The triggering of bioweathering mechanisms, namely, the upregulation of genes involved in carbonate ion production from CO_2 in the presence of silicate minerals, was reported for another Ascomycete fungus (*Aspergillus fumigatus*; Xiao et al., 2012). This study and others (e.g., Olsson-Francis et al., 2010; Kirtzel et al., 2017) further support the conclusion that microbial weathering processes play a role in the determination of accurate fluxes of carbon and bioavailable nutrients in the critical zone.

Overall, our study demonstrates that local weathering rates can be determined *in situ* while identifying the actors involved in microbially mediated dissolution and quantifying their effect on weathering fluxes. The proposed approach can be extended to probe the bioweathering potential of a virtually unlimited range of natural environments as well as in sensitive industrial contexts, for which knowledge of the microbial contribution to corrosion and silicate weathering is not only fundamental but also urgently needed (Trias et al., 2017). The incubation of mineral probes *in situ* provides the reference kinetic parameters and microbial data required to set up a next generation of RTMs accounting for microbially mediated mineral dissolution. Gradual inclusion of microbial dynamics in RTMs constitutes an important milestone in modeling the biosphere and its impact on regolith (Goddéris et al., 2019). Beyond providing a quantitative assessment of bioweathering rates, the proposed approach is also well suited to identify biosignatures on material surfaces, which is a prerequisite to confirm the biotic contribution to dissolution and unravel underlying bioweathering mechanisms.

Other OTUs (<3%) 25%

Other (Fungi) 26%

Verticillium 4%

Mortierella 12%

Enrichment factor 0 — 100

Hydnotrya 14%
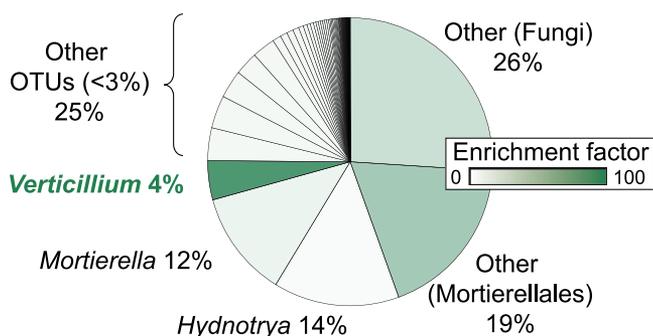
Other (Mortierellales) 19%

Figure 3. Relative abundance of fungal genera associated with olivine samples and enrichment compared to relative abundance in soil. OTUs—Operational Taxonomic Units.

REFERENCES CITED

Ahmed, E., and Holmstrom, S.J.M., 2015, Microbe-mineral interactions: The impact of surface attachment on mineral weathering and element selectivity by microorganisms: Chemical Geology, v. 403, p. 13–23, https://doi.org/10.1016/j.chemgeo.2015.03.009.

Al-Bulushi, I.M., Bani-Uraba, M.S., Guizani, N.S., Al-Khusaibi, M.K., and Al-Sadi, A.M., 2017, Illumina MiSeq sequencing analysis of fungal diversity in stored dates: BMC Microbiology, v. 17, p. 72, https://doi.org/10.1186/s12866-017-0985-7.

Banfield, J.F., Barker, W.W., Welch, S.A., and Taunton, A., 1999, Biological impact on mineral dissolution: Application of the lichen model to understanding mineral weathering in the rhizosphere: Proceedings of the National Academy of Sciences of the United States of America, v. 96, p. 3404–3411, https://doi.org/10.1073/pnas.96.7.3404.

Beerling, D.J., et al., 2020, Potential for large-scale CO_2 removal via enhanced rock weathering with croplands: Nature, v. 583, p. 242–248, https://doi.org/10.1038/s41586-020-2448-9.

Benzerara, K., Yoon, T.H., Menguy, N., Tyliszczak, T., and Brown, G.E., 2005, Nanoscale environments associated with bioweathering of a Mg-Fe-pyroxene: Proceedings of the National Academy of Sciences of the United States of America, v. 102, p. 979–982, https://doi.org/10.1073/pnas.0409029102.

Bonneville, S., Morgan, D.J., Schmalenberger, A., Bray, A., Brown, A., Banwart, S.A., and Benning, L.G., 2011, Tree-mycorrhiza symbiosis accelerate mineral weathering: Evidences from nanometer-scale elemental fluxes at the hypha-mineral interface: Geochimica et Cosmochimica Acta, v. 75, p. 6988–7005, https://doi.org/10.1016/j.gca.2011.08.041.

Bonneville, S., Smits, M.M., Brown, A., Harrington, J., Leake, J.R., Brydson, R., and Benning, L.G., 2009, Plant-driven fungal weathering: Early stages of mineral alteration at the nanometer scale: Geology, v. 37, p. 615–618, https://doi.org/10.1130/G25699A.1.

Brantley, S., Megonigal, J.P., Scatena, F., Balogh-Brunstad, Z., Barnes, R., Bruns, M., Van Cappellen, P., Dontsova, K., Hartnett, H., and Hartshorn, A., 2011, Twelve testable hypotheses on the geobiology of weathering: Geobiology, v. 9, p. 140–165, https://doi.org/10.1111/j.1472-4669.2010.00264.x.

Daghino, S., Turci, F., Tomatis, M., Girlanda, M., Fubini, B., and Perotto, S., 2009, Weathering of chrysotile asbestos by the serpentine rock–inhabiting fungus *Verticillium leptobactrum*: FEMS Microbiology Ecology, v. 69, p. 132–141, https://doi.org/10.1111/j.1574-6941.2009.00695.x.

Drever, J., and Stillings, L., 1997, The role of organic acids in mineral weathering: Colloids and Surfaces A—Physicochemical and Engineering Aspects, v. 120, p. 167–181, https://doi.org/10.1016/S0927-7757(96)03720-X.

Fischer, C., and Luttge, A., 2018, Pulsating dissolution of crystalline matter: Proceedings of the National Academy of Sciences of the United States of America, v. 115, p. 897–902, https://doi.org/10.1073/pnas.1711254115.

Frings, P.J., and Buss, H.L., 2019, The central role of weathering in the geosciences: Elements, v. 15, p. 229–234, https://doi.org/10.2138/gselements.15.4.229.

Gerrits, R., Wirth, R., Schreiber, A., Feldmann, I., Knabe, N., Schott, J., Benning, L.G., and Gorbushina, A.A., 2021, High-resolution imaging of fungal biofilm-induced olivine weathering: Chemical Geology, v. 559, p. 119902, https://doi.org/10.1016/j.chemgeo.2020.119902.

Gleeson, D.B., Clipson, N., Melville, K., Gadd, G.M., and McDermott, F.P., 2005, Characterization of fungal community structure on a weathered pegmatitic granite: Microbial Ecology, v. 50, p. 360–368, https://doi.org/10.1007/s00248-005-0198-8.

Goddéris, Y., Schott, J., and Brantley, S.L., 2019, Reactive transport models of weathering: Elements, v. 15, p. 103–106, https://doi.org/10.2138/gselements.15.2.103.

Hazen, R.M., Papineau, D., Bleeker, W., Downs, R.T., Ferry, J.M., McCoy, T.J., Sverjensky, D.A., and Yang, H., 2008, Mineral evolution: The American Mineralogist, v. 93, p. 1693–1720, https://doi.org/10.2138/am.2008.2955.

Hellmann, R., Wirth, R., Daval, D., Barnes, J.-P., Penisson, J.-M., Tisserand, D., Epicier, T., Florin, B., and Hervig, R.L., 2012, Unifying natural and laboratory chemical weathering with interfacial dissolution–reprecipitation: A study based on the nanometer-scale chemistry of fluid-silicate interfaces: Chemical Geology, v. 294–295, p. 203–216, https://doi.org/10.1016/j.chemgeo.2011.12.002.

Jones, A.A., and Bennett, P.C., 2014, Mineral microniches control the diversity of subsurface microbial populations: Geomicrobiology Journal, v. 31, p. 246–261, https://doi.org/10.1080/01490451.2013.809174.

Kirtzel, J., Siegel, D., Krause, K., and Kothe, E., 2017, Stone-eating fungi: Mechanisms in bioweathering and the potential role of laccases in black slate degradation with the basidiomycete *Schizophyllum* commune, *in* Sariaslani, S., and Gadd, G.M., eds., Advances in Applied Microbiology, Volume 99: San Diego, California, Academic Press, p. 83–101, https://doi.org/10.1016/bs.aambs.2017.01.002.

Knowles, E., Wirth, R., and Templeton, A., 2012, A comparative analysis of potential biosignatures in basalt glass by FIB-TEM: Chemical Geology, v. 330–331, p. 165–175, https://doi.org/10.1016/j.chemgeo.2012.08.028.

Li, Z., Liu, L., Chen, J., and Teng, H.H., 2016, Cellular dissolution at hypha- and spore-mineral interfaces revealing unrecognized mechanisms and scales of fungal weathering: Geology, v. 44, p. 319–322, https://doi.org/10.1130/G37561.1.

Meile, C., and Scheibe, T.D., 2019, Reactive transport modeling of microbial dynamics: Elements, v. 15, p. 111–116, https://doi.org/10.2138/gselements.15.2.111.

Mitchell, A.C., Lafreniere, M.J., Skidmore, M.L., and Boyd, E.S., 2013, Influence of bedrock mineral composition on microbial diversity in a subglacial environment: Geology, v. 41, p. 855–858, https://doi.org/10.1130/G34194.1.

Napieralski, S.A., Buss, H.L., Brantley, S.L., Lee, S., Xu, H., and Roden, E.E., 2019, Microbial chemolithotrophy mediates oxidative weathering of granitic bedrock: Proceedings of the National Academy of Sciences of the United States of America, v. 116, p. 26394–26401, https://doi.org/10.1073/pnas.1909970117.

Olsson-Francis, K., Van Houdt, R., Mergeay, M., Leys, N., and Cockell, C.S., 2010, Microarray analysis of a microbe-mineral interaction: Geobiology, v. 8, p. 446–456, https://doi.org/10.1111/j.1472-4669.2010.00253.x.

Pierret, M.-C., et al., 2018, The Strengbach catchment: A multidisciplinary environmental sentry for 30 years: Vadose Zone Journal, v. 17, p. 180090, https://doi.org/10.2136/vzj2018.04.0090.

Rogers, J.R., and Bennett, P.C., 2004, Mineral stimulation of subsurface microorganisms: Release of limiting nutrients from silicates: Chemical Geology, v. 203, p. 91–108, https://doi.org/10.1016/j.chemgeo.2003.09.001.

Schwartzman, D.W., and Volk, T., 1989, Biotic enhancement of weathering and the habitability of Earth: Nature, v. 340, p. 457–460, https://doi.org/10.1038/340457a0.

Trias, R., et al., 2017, High reactivity of deep biota under anthropogenic CO_2 injection into basalt: Nature Communications, v. 8, p. 1063, https://doi.org/10.1038/s41467-017-01288-8.

Uroz, S., Kelly, L.C., Turpault, M.-P., Lepleux, C., and Frey-Klett, P., 2015, The mineralosphere concept: Mineralogical control of the distribution and function of mineral-associated bacterial communities: Trends in Microbiology, v. 23, p. 751–762, https://doi.org/10.1016/j.tim.2015.10.004.

van Schöll, L., Kuyper, T.W., Smits, M.M., Landeweert, R., Hoffland, E., and Van Breemen, N., 2008, Rock-eating mycorrhizas: Their role in plant nutrition and biogeochemical cycles: Plant and Soil, v. 303, p. 35–47, https://doi.org/10.1007/s11104-007-9513-0.

Velbel, M.A., 2009, Dissolution of olivine during natural weathering: Geochimica et Cosmochimica Acta, v. 73, p. 6098–6113, https://doi.org/10.1016/j.gca.2009.07.024.

Wild, B., Imfeld, G., Guyot, F., and Daval, D., 2018, Early stages of bacterial community adaptation to silicate aging: Geology, v. 46, p. 555–558, https://doi.org/10.1130/G40283.1.

Wild, B., Daval, D., Beaulieu, E., Pierret, M.-C., Viville, D., and Imfeld, G., 2019, In-situ dissolution rates of silicate minerals and associated bacterial communities in the critical zone (Strengbach catchment, France): Geochimica et Cosmochimica Acta, v. 249, p. 95–120, https://doi.org/10.1016/j.gca.2019.01.003.

Xiao, B., Lian, B., Sun, L., and Shao, W., 2012, Gene transcription response to weathering of K-bearing minerals by *Aspergillus fumigatus*: Chemical Geology, v. 306–307, p. 1–9, https://doi.org/10.1016/j.chemgeo.2012.02.014.

Printed in USA